This is a repository copy of *On the correct estimation of the magnetic entropy change across the magneto-structural transition from the Maxwell relation: Study of MnCoGeBx alloy ribbons*.

White Rose Research Online URL for this paper:
http://eprints.whiterose.ac.uk/107684/

Version: Accepted Version

Accepted Manuscript

On the correct estimation of the magnetic entropy change across the magneto-structural transition from the Maxwell relation: Study of MnCoGeB$_x$ alloy ribbons

A. Quintana-Nedelcos, J.L. Sánchez Llamazares, C.F. Sánchez-Valdés, P. Álvarez Alonso, P. Gorria, P. Shamba, N.A. Morley

Please cite this article as: A. Quintana-Nedelcos, J.L. Sánchez Llamazares, C.F. Sánchez-Valdés, P. Álvarez Alonso, P. Gorria, P. Shamba, N.A. Morley, On the correct estimation of the magnetic entropy change across the magneto-structural transition from the Maxwell relation: Study of MnCoGeB$_x$ alloy ribbons, *Journal of Alloys and Compounds* (2016), doi: 10.1016/j.jallcom.2016.10.116.

On the correct estimation of the magnetic entropy change across the magneto-structural transition from the Maxwell relation: study of MnCoGeB$_x$ alloy ribbons

A. Quintana-Nedelcos [a,f,*], J.L. Sánchez Llamazares [b,**], C.F. Sánchez-Valdés [c], P. Álvarez Alonso [d], P. Gorria [e], P. Shamba [f], N. A. Morley [f]

[a] *Department of Metallurgical and Materials Engineering, Marmara University, 34722 Istanbul, Turkey*
[b] *Instituto Potosino de Investigación Científica y Tecnológica A.C., Camino a la Presa San José No 2055, Col. Lomas 4ª sección, San Luis Potosí, S.L.P. 78216, México*
[c] *División Multidisciplinaria, Ciudad Universitaria, Universidad Autónoma de Ciudad Juárez (UACJ), calle José de Jesús Macías Delgado # 18100, Ciudad Juárez 32579, Chihuahua, México*
[d] *Departamento de Electricidad y Electrónica, Universidad del País Vasco (UPV/EHU), 48940 Leioa, Spain.*
[e] *Departamento de Física, EPI, Universidad de Oviedo, Gijón, 33203, Spain*
[f] *Department of Materials Science and Engineering, University of Sheffield, Sheffield S1 3JD, United Kingdom*

ABSTRACT. An accurate calculation of the different magnetocaloric-related magnitudes derived from the temperature dependence of the magnetic entropy change in materials exhibiting first-order magnetocaloric effect is imperative to correctly estimate the true potential of a specific material for refrigeration purposes. In this contribution, we present a meticulous study of two different thermal procedures to measure the set of isothermal magnetization curves from which the total field induced magnetic entropy change, ΔS_T, is calculated using the adequate Maxwell relation. If the accurate determination of ΔS_T for any temperature is pursued the thermal and magnetic history of the materials must be taken into account, and then, the unidirectional measurement of reversible isothermal magnetization curves after a thermal cycle is required. The analysis was conducted on MnCoGeB$_{0.01}$ alloy ribbons that show a giant ΔS_T at the coupled magneto-structural transition, from a ferromagnetic (TiNiSi-type) phase to a paramagnetic (NiIn$_2$-type) one, owing to the concomitant abrupt magnetization change. We suggest that the conclusions reached can be applicable to any other system displaying magnetocaloric effect originated at a first-order phase transition.

* Corresponding author. Department of Materials Science and Engineering, University of Sheffield, Sheffield S1 3JD, United Kingdom. E-mail addresses: a.quintana-nedelcos@sheffield.ac.uk and arisqn@gmail.com

** Corresponding author. Instituto Potosino de Investigación Científica y Tecnológica A.C., Camino a la Presa San José 2055 Col. Lomas 4ª sección, San Luis Potosí 78216, San Luis Potosi, México. E-mail addresses: jose.sanchez@ipicyt.edu.mx

1. Introduction

Since the giant magnetocaloric effect (GMCE) was reported in the $Gd_5(Si_2Ge_2)$ alloy in 1997 [1], some discrepancies between authors about the correct determination of the temperature dependence of the total magnetic entropy change $\Delta S_T(T)$ from isothermal magnetization measurements for materials exhibiting GMCE have emerged. The main controversial point refers to the validity of the Maxwell relation (equation 1) [2-6], in the sense that the appropriate selection of the thermal procedure to measure a set of isothermal magnetization curves $M(\mu_oH)$ is of paramount importance for a correct estimation of the $\Delta S_T(T)$ curve [7-10]:

$$\left(\frac{\partial S}{\partial B}\right)_T = \left(\frac{\partial M}{\partial T}\right)_B \quad \rightarrow \quad \Delta S_T(T, \Delta B) = \int_0^{B_{max}} \left[\frac{\partial M(T,B')}{\partial T}\right]_{B'} dB' \qquad (1)$$

The determination of the magnetic entropy change from isothermal magnetization curves, $M(\mu_oH)$, through the Maxwell relation for materials undergoing a second order phase transition (SOPT) is well established. In these systems, apart from considering the effect of the demagnetizing field (i.e., $\mu_oH_{int} = \mu_oH_{ext} - N_dM$), that entails the sample preparation with the appropriate geometry to perform the proper correction on the $M(\mu_oH)$ curves, a particular care must be paid in order to assure that for each temperature the measurement of the $M(\mu_oH)$ curve must start with the sample in the thermally demagnetized state. The magnetization isothermal curves can be successively measured either on heating or cooling. However, for a material exhibiting a first order phase transition (FOPT) the magneto-thermal history followed prior to measure successive isothermal $M(\mu_oH)$ curves around the coupled field-induced magneto-structural transition is the origin of discrepancies on the estimated value of $\Delta S_T(T)$ [11]. The GMCE shown in FOPT materials is explained under the consideration that the value of ΔS_T is the sum of the conventional second order magnetic entropy change, ΔS_M, and the entropy difference between the two different crystallographic polymorphs, ΔS_{st}, [12-14]. In this sense, most of the discussion focuses on the overestimation of ΔS_T when is calculated from the isothermal magnetization curves that sometimes gives rise to a spike-like shape of the $\Delta S_T(T)$ curves. The origin of the spike has been considered as an artefact due to the summation of the Maxwell relation with a finite field interval [2]. Liu *et al*. [3] suggested that the spurious spike comes from the inadequate use of the Maxwell relation within the temperature region of the magneto-structural transition, where the paramagnetic (PM) and ferromagnetic (FM) phases coexist. Moreover, it has been stated that the height of the spurious spike is inversely proportional to the temperature step ΔT between two subsequent isothermal $M(\mu_oH)$ curves and proportional to the variation of the molar fraction between T and $T + \Delta T$ [5]. A thermal procedure (referred as LOOP procedure, that we describe below) was suggested by

2

Caron *et al*. [9] as a practical method to almost avoid the spurious spike-like shape of the $\Delta S_T(T)$ curves. However, the $\Delta S_T(T)$ curve becomes broader and, as a result, the area below the $\Delta S_T(T)$ curve is essentially the same independently of the thermal procedure [15]. More recently, the results obtained from different procedures in a $Ni_{50}Mn_{28}Ga_{22}$ single crystal by Niemann *et al*. reveal that the LOOP procedure approach fails due to the magnetically induced reorientation of the crystal structure in the martensitic phase [10]. In addition to the spike effect, the contribution due to the irreversibility of the process should be taken into consideration for an accurate estimation of ΔS_T.

Diverse families of materials exhibiting FOPT have been investigated as potential candidates for room temperature magnetic refrigeration applications. Among them, $Gd_5(Si_xGe_{1-x})_4$ [1, 16], $La(Si,Fe,X)_{13}$ (X= Co, Mn) [17, 18], MnFe(P,X) with X = As, Ge, Si [6, 19], non-stoichiometric Ni-Mn-X-based Heusler-type (X= Ga, Sn, In, Sb) [20-26] or Mn(Co,Ni)Ge-based alloys [27-37]. It is worth noting that MnCoGe-based alloys have one of the largest contributions of ΔS_{st} to ΔS_T, giving rise to one of the highest reported GMCE in terms of the maximum value of ΔS_T [14]. The coupled magneto-structural transition in these alloys occurs between the PM hexagonal (hex) parent phase (Ni_2In-type crystal structure; space group P6$_3$/*mmc*) and the FM low temperature orthorhombic (orth) phase (TiNiSi-type crystal structure; space group *Pnma*) [38, 39]. This transition is attained when the starting and finishing temperatures for the direct and reverse martensitic transformation M_S, M_f, A_f, and A_S, respectively, are within the temperature window delimited by the Curie temperature of the hexagonal (T_C^{hex}) and orthorhombic (T_C^{orth}) phases [32, 38]. These phases are often called austenite (AST) and martensite (MST), respectively.

The effect of B on the crystal structure, magnetization behaviour and martensitic transformation in the MnCoGeB$_x$ (0.01 ≤ x ≤ 0.05) system was first reported by Trung et al., assuming that boron atoms occupy interstitial sites [32, 40]. They found that the addition of B provokes a drastic shift of the FOPT temperature from about 650 K for the stoichiometric MnCoGe alloy, to be tuned around room temperature (between the T_C values of the two allotropic MnCoGe phases) [41, 42], whereas the magnetic moment per formula unit remains unaffected (3.86-3.85 μ_B/f.u.) for 0.01 ≤ x ≤ 0.03. Moreover, the maximum value of the magnetic entropy change reaches values of 38-47 $Jkg^{-1}K^{-1}$ for x = 0.02, 0.03. The structural transition is accompanied by a large relative volume change, estimated as ~ 2.3 % for x = 0.02 [40], and around 4.0 % for other MnCoGe-based alloys [39, 41]; as stated by Pecharsky et al. [14], MnCoGeB$_x$ alloys with x = 0.02, 0.03 show the largest contribution from ΔS_{st} to ΔS_T. An important feature of these alloys, closely related to our investigation, is that the magnetic field induces the AST-to-MST phase transition [43], being the lattice defects

3

originated by the interstitial inclusion of boron atoms the key ingredient that facilitates the nucleation and growth of the martensitic low-temperature phase in the $MnCoGeB_x$ system [38].

In this work we discuss about the differences in the magnetic entropy change vs. temperature curve as well as in the refrigerant capacity RC of $MnCoGeB_{0.01}$ alloy ribbons obtained from the widely used LOOP procedure [9], and from the herein described BnF ("Back and Forward") heating-cooling procedure. The observed discrepancies depend on the thermomagnetic history of the sample.

2. Experimental procedures

A 3 g bulk alloy sample with nominal composition $MnCoGeB_{0.01}$ ($Mn_{29.44}Co_{31.58}Ge_{38.92}B_{0.06}$ and ($Mn_{33.22}Co_{33.22}Ge_{33.22}B_{0.34}$ in molar % and at. %, respectively) was prepared by argon arc melting from highly pure starting elements (Mn 99.9998 %, Ge 99.9999 %, Co 99.98 % and B 99.6 %). The sample was melted 3 times to ensure a good starting chemical homogeneity. As-spun ribbons were obtained by melt spinning under a controlled ultra-highly pure argon environment. The linear speed of the rotating copper wheel was kept constant at 20 ms^{-1}. To ensure an homogeneous crystalline structure, the ribbons were encapsulated in quartz tubes under an ultra-highly pure argon atmosphere and annealed for 4 hours at 1148 K and then were water quenched. The average dimensions of the obtained ribbon flakes were around 30-35 µm thick, 8-15 mm length and 1.2-1.5 mm width.

The phase transitions occurring in the sample were investigated by differential scanning calorimetry (DSC) using a TA Instruments model Q200 system. X-ray diffraction (XRD) patterns of finely powdered samples were collected at room temperature with a Rigaku smartlab high-resolution diffractometer using Cu-Kα radiation (λ = 1.5418 Å; $20^o \leq 2\theta \leq 60^o$; step increment 0.01^o). Magnetization measurements were performed using a Quantum Design Evercool-I PPMS 9T platform with the vibrating sample magnetometer module. The $\Delta S_T(T)$ curves were obtained from a set of $M(\mu_o H)$ isotherms by applying the Maxwell relation (equation 1). Refrigerant capacity (RC) was estimated making use of the following three different criteria: $RC\text{-}1 = |\Delta S_T^{peak}| \times \delta T_{FWHM}$, $RC-2 = \int_{T_{cold}}^{T_{hot}} [\Delta S_T(T)]_{\mu_o H} dT$, and RC-3 according to the Wood and Potter method [44]. In case of RC-1 and RC-2, δT_{FWHM} is the temperature interval corresponding to the full-width at half-maximum of the $\Delta S_T(T)$ curve that is delimited by the temperatures T_{hot} and T_{cold}. $\delta T_{FWHM} = T_{hot} - T_{cold}$ is usually assumed as the useful working temperature range of the magnetic refrigerant. We shall focus our attention on the estimation of the magnetic entropy change associated to the *on heating* phase transition

(i.e., from the ortho-FM to the hex-PM phase). The two different thermal procedures (TP) we have considered are the following:

TP-1 (LOOP procedure): firstly, the sample is cooled down to the selected starting temperature, T_1; (i) the isothermal $M(\mu_o H)$ curve is measured at $T = T_1$ under an increasing applied magnetic field from 0 to $\mu_o H^{max}$; (ii) the magnetic field is removed; (iii) the sample is heated up to a temperature at which the sample is in PM state; (iv) the sample is cooled down to the next selected temperature, $T_2 = T_1 + \Delta T$. Then, the procedure is repeated, following steps (i) to (iv), up to the final selected temperature to acquire the full set of isothermal $M(\mu_o H)$ curves within the target temperature range.

TP-2 (BnF procedure): After selecting the starting temperature, T_1, we follow steps (i), (ii) and (iii) of the TP-1 procedure. However, the main difference in BnF procedure is the subsequent cooling of the sample that now goes down to a temperature well below the structural phase transformation M_f, where the sample is in FM state. Afterwards, the sample is heated to the next measuring temperature $T_2 = T_1 + \Delta T$ and the procedure is repeated up to the final selected temperature. The key point here is the following: TP-2 procedure ensures that the sample always reaches each selected measuring temperature through the same thermal and magnetic history; and therefore, the phase percentages across the phase transition region is that given by the DSC curve.

3. Results and discussion

Figures 1(a) and 2(a) show the heating/cooling DSC curves for $MnCoGeB_{0.01}$ ribbon samples, whereas the magnetization vs. temperature curves measured under a low magnetic field (5 mT) on heating after zero-field-cooling, $M_{ZFC}(T)$, and during field-cooling, $M_{FC}(T)$, are depicted in Figures 1(b) and 2(b). From calorimetric curves the temperatures associated with the direct and reverse martensitic transformations can be obtained: $A_S = 318$ K, $A_f = 343$ K, $M_S = 313$ K and $M_f = 282$ K. The coupling between the structural and magnetic transitions, between the FM-orth phase and the PM-hex phase, is clearly evidenced in DSC and $M(T)$ curves, being consistent with those already reported [32, 45-47].

In Figure 3 we plot two different room temperature X-ray powder diffraction patterns of the sample. The pattern in figure 3(a) corresponds to a ribbon that was previously heated up to 1148 K, and that in figure 3(b) to a ribbon cooled down to 77 K and subsequently taken to RT. Both patterns show the coexistence of the hexagonal (H) Ni_2In-type and the orthorhombic (O) TiNiSi-type phases with the expected volume fraction at RT from DSC and $M(T)$ measurements. There is not any evidence of secondary or spurious phases.

5

We have selected the MST → AST transition, i.e. the magneto-structural transition from the FM-orth phase to the PM-hex phase, in order to obtain the $\Delta S_T(T)$ curves in the MnCoGeB$_{0.01}$ ribbon sample. By choosing this transition direction, the reported magnetic field induced effect of the PM-hex to the FM-ortho phase transition [38, 42] can be avoided, and therefore, only the magneto-structural transition contributes to the $\Delta S_T(T)$. In Fig. 1(c) and Fig. 2(c) we show the obtained $\Delta S_T(T)$ curves from TP-1 and TP-2 procedures, respectively. The main differences between both curves are related with the maximum value of the total entropy change, ΔS_T^{peak}, and the temperature for this maximum. These discrepancies depend on the different thermo-magnetic procedure used for measuring the set of isothermal magnetization curves. We will discuss now the results from both procedures in more detail:

TP-1 (Figure 1): Let's assume that the temperature corresponding to point 1 (red solid circle number 1) is chosen to measure the first isothermal $M(\mu_o H)$ curve. After the measurement, the sample is heated up to a temperature well above M_S (to ensure a complete AST-PM state). Then, it is cooled down to the next measuring temperature, namely point 2 (red solid circle number 2$_i$). Unlike point 1, point 2$_i$ belongs to the cooling path of the calorimetric and $M(T)$ curves that appear in figure 1(a) and figure 1(b), respectively. If the $M(\mu_o H)$ curve is measured increasing the magnetic field from 0 to $\mu_o H^{\text{max}}$, the sample undergoes a field-induced phase transition (FIPT) from the PM-hex phase to the FM-orth phase [38, 42]. However, in the backward direction (i.e., from orth to hex phase) no FIPT exists; accordingly, when the applied magnetic field is removed the transformed phase fraction remains (solid rhombus labelled as 2$_f$ in figure 1(a) and 1(b)). As a result, after each applied/removed magnetic field cycle there is an extra contribution to the total magnetic entropy change due to the field-induced AST → MST. It is worth noting that the amount of transformed phase due to the FIPT effect cannot be larger than the volume fraction in the PM-hex phase for the temperature at which the isothermal curve is measured. Thus, it is reasonable to find ΔS_T^{peak} at point 2 since the maximum contribution due to the FIPT occurs at this temperature. On cooling below this temperature (i.e., that of point 2), the fraction of FM-orth phase in the initial state increases, leading to a lower contribution of the FIPT from PM-hex to the FM-orth phase (with the lower limit at point 1). For temperatures above that corresponding to the ΔS_T^{peak} (point 2) the PM-hex phase increases, giving rise to a lower contribution of the FIPT from PM-hex to the FM-orth phase (with the upper limit at point 3).

TP-2 (Figure 2): We follow the same steps of TP-1 procedure until the heating up to $T > M_S$ (to ensure again a complete AST-PM state), but then, the sample is cooled down to $T < A_S$ in order to guarantee that the sample is in MST-FM state before heating it up to the next measuring temperature (point 2). The process is repeated after every isothermal magnetization curve is completed. By means

of this thermal procedure the sample reaches every measurement temperature following the same thermal and magnetic history. Notice that the temperature interval for the ΔS_T curve corresponds to that of the MST to AST magneto-structural transition; this is denoted by the vertical white stripe depicted in figure 2. The temperature corresponding with the position of ΔS_T^{peak} (point 2) is in excellent agreement with the DSC [minimum of the heating curve within the MST-to-AST transition, see figure 2(a)] and the $M(T)$ curve [inflection point in figure 2(a)].

From now on we will refer to the ΔS_T^{peak} temperature for both thermal procedures as T_{ms}. At this temperature the contribution of the field-induced magneto-structural transition to the total entropy change is maximum, but its origin is different for TP-1 and TP-2.

The measured $M(\mu_o H)$ curves for TP-1 and TP-2 are depicted in figures 4(a) and (c), respectively. The monotonous increment of magnetization on increasing the applied magnetic field with a non-saturating trend [see figure 4(a)] results from the FIPT effect when TP-1 is used. This is further confirmed by the irreversible behaviour, or magnetic hysteresis, observed between the isothermal $M(\mu_o H)$ curves measured following an increasing-decreasing magnetic field cycle [see figure 4(b)]. When TP-1 is used, the maximum magnetic hysteretic loss (18 %) is achieved at T_{ms} = 316 K. In contrast, figure 4(c) shows that for TP-2 the isothermal $M(\mu_o H)$ curves tend to saturate in the ferromagnetic region. In this case, T_{ms} = 331 K. Moreover, the field-up and field-down $M(\mu_o H)$ curves overlap (absence of hysteresis) owing to the absence of any field induced magneto-structural transformation [see figure 4(d)].

The isothermal magnetization curves obtained following TP-1 are smooth and exhibit a monotonous dependence on the applied magnetic field instead of a step-like shape typical for materials with a critical activation field due the FIPT effect at a given temperature [7], in which once the FIPT is completed the structural contribution to the entropy change remains magnetic field independent [37]. Hence, the shape of the $M(\mu_o H)$ curves does not depend only on the thermal procedure [9], but also on the nature of the FIPT (i.e., step-like or monotonous with the applied magnetic field), if it exists. Thus, the spike effect arises as an artefact of the Maxwell relation (equation *1*) when ΔS_T is obtained from step-like $M(\mu_o H)$ curves. ΔS_T curves with gaussian-like shape are obtained from smoothly monotonous $M(\mu_o H)$ curves, and give no information on the existence or absence of any FIPT phenomenon. For example, no spike effect is achieved when both TP-1 and TP-2 are used, figure 1(c) and figure 2(c), respectively, even though the FIPT effect was proven to occur when the PT-1 is used.

It is worth noting that the dissipative energy E_d, related to the irreversibility of the process, should be subtracted from the area below the $\Delta S_T(T)$ curve for a correct estimation of the GMCE in materials exhibiting FIPT. E_d can be estimated from isothermal magnetization measurements, where E_d is one half of the area enclosed by the loop at each temperature [14]. Following this method, we have calculated the energy losses (due to the E_d), being around 9 % at $T_{ms} = 316$ K for TP-1 [see figure 4(b)], and $E_d \sim 12$ % when the contribution of all the loops is added. Surprisingly, the difference between the areas below ΔS_T curves obtained from TP-1 and TP-2 is of the same order: Area(ΔS_T; TP-1) - Area(ΔS_T; TP-2) = 11 %.

From the application standpoint, the calculation of the refrigerant capacity, RC, is a relevant parameter for evaluating the quality of magnetic refrigerants. The RC gives the effective amount of heat that might be transferred from the hot to the cold sink if an ideal refrigeration cycle is considered; its magnitude is proportional to the area below the $\Delta S_T(T)$ curve. Figure 5 shows the calculated RC-1, RC-2 and RC-3 up to a maximum magnetic field change of $\mu_o\Delta H = 5$ T. In Table 1 the RC values for $\mu_o\Delta H = 2$ T and 5 T estimated from experimental data following TP-1 and TP-2 procedures, as well as the differences in percentage between them are given. Notice that the overestimation of the RC values from the TP-1 data is again of the order of the calculated irreversible isothermal losses, because it depends directly on the area below ΔS_T curve as mentioned above. In accordance with reference [47], the effect corresponding to the magnetic entropy change due to the FIPT has the same sign as that of the martensitic structural transition, giving rise to an enhancement of the magnetocaloric effect.

In addition, if we compare the direct measurement of the magnetization curves obtained from an isofield measurement under 5 T (solid circles in figure 6) and those obtained indirectly from isothermal data following TP-1 (open squares in figure 6) and TP-2 (open circles in figure 6) the result should be equivalent because both isofield and isothermal measurements probe the same phenomenon [9]. The direct $M(T)$ measurement is in good agreement with the curve obtained from TP-2. Once again, we can conclude that using TP-2 is the correct way to ensure that the transition is being traversed in the same way.

We have demonstrated, by using MnCoGeB$_{0.01}$ as a case of study, that the magnetocaloric properties of a material estimated from isothermal magnetization measurements can be miscalculated if a wrong thermal procedure is used. However, the reader must note that: (a) rather than a distinctive characteristic of the MnCoGeB$_x$ alloys, the occurrence of field-induced phase transitions, together with the associated irreversibility, is a common feature of most of the magnetocaloric materials already

known exhibiting a giant field-induced magnetic entropy change (i.e. GMCE, owing to a coupled FOPT); (b) the application of Maxwell relation is the most common method followed by the scientific community to estimate the temperature dependence of ΔS_T. The thermal procedure here described (BnFHC) allows an accurate and reliable determination of $\Delta S_T(T)$. Its implementation must start after the starting and finishing FOPT temperatures are precisely determined, typically by DSC and low-field $M(T)$ measurements. Afterwards, the transition path to be investigated and the most adequate thermal procedure to measure each isothermal magnetization curve in the temperature interval of the FOPT must be selected. This supports our view that the procedure here presented could be universally applied to any other first-order magnetocaloric effect system.

4. Conclusions

In summary, we have investigated and analyzed the effect that two different thermal procedures have on the calculated isothermal magnetic entropy change and the refrigerant capacity in $MnCoGeB_{0.01}$ alloy ribbons from magnetization curves. We found that even though an overestimation of the magnetocaloric effect of a material is usually shown as a spike in the magnetic entropy change curve, the absence of it doesn't imply that both the maximal entropy change and the refrigerant capacity are undoubtedly properly determined. We demonstrated that the MCE parameters (as: ΔS_T^{peak} value and position, the area below ΔS_T curve, and the refrigerant capacity) are strongly dependent on the thermal procedure employed during the measurement. This should take into consideration the thermal and magnetic history of the sample. Thus, for a correct estimation of the magnetic entropy change in the absence of the FIPT effect, the isothermal measurements should be always performed across the same direction of the transition. Otherwise, there is a risk of measuring the FIPT effect of the reversal transition, if any.

Acknowledgement

9

References

[1] V.K. Pecharsky, K.A. Gschneidner, Phys. Rev. Lett. 78 (1997) 4494.

[2] H. Wada, Y. Tanabe, Appl. Phys. Lett. 79 (2001) 3302.

[3] G. J. Liu, J. R. Sun, J. Shen, B. Gao, H.W. Zhang, F.X. Hu, B. G. Shen, Appl. Phys. Lett. 90, (2007) 032507.

[4] N.A de Oliveira, P.J. von Ranke, Phys. Rev. B 77 (2008) 214439.

[5] L. Tocado, E. Palacios, R. Burriel, J. Appl. Phys. 105 (2009) 093918.

[6] P. Yibole, F. Guillou, N.H. van Dijk, E. Brück, J. Phys. D. Appl. Phys. 47 (2014) 075002.

[7] A.M.G. Carvalho, A.A. Coelho, S. Gama, P.J. von Ranke, C.S. Alves, J. Appl. Phys. 104 (2008) 063915.

[8] A.M.G. Carvalho, A.A. Coelho, P.J. von Ranke, C.S. Alves, J. Alloys Compd. 509 (2011) 3452.

[9] L. Caron, Z.Q. Ou, T.T. Nguyen, D.T. Cam Thanh, O. Tegus, E. Brück, J. Magn. Magn. Mater. 321 (2009) 3559.

[10] R. Niemann, O. Heczko, L. Schultz, S. Fähler, Int. J. Refrig. 37 (2014) 281.

[11] M. Bratko, K. Morrison, A. De Campos, S. Gama, L.F. Cohen, K.G. Sandeman, Appl. Phys. Lett. 100 (2012) 252409.

[12] K.A. Gschneidner Jr, V.K. Pecharsky, O. Tsokol, Reports Prog. Phys. 68 (2005) 1479.

[13] V.K. Pecharsky, A.P. Holm, K.A. Gschneidner, R. Rink, Phys. Rev. Lett. 91 (2003) 197204.

[14] K.A. Gschneidner Jr., Y. Mudryk, V.K. Pecharsky, Scripta Mater. 67 (2012) 572.

[15] G.F. Wang, Magnetic and Calorimetric Study of the Magnetocaloric Effect in Intermetallics Exhibiting First-order Magnetostructural Transitions, Universidad de Zaragoza, (2012) PhD Thesis.

[16] V.K. Pecharsky, K.A. Gschneidner, Adv. Mater. 13 (2001) 683.

[17] X.B Liu, Z. Altounian, J. Magn. Magn. Mater. 264 (2003) 209.

[18] K. Morrison, K.G. Sandeman, L.F. Cohen, C.P. Sasso, V. Basso, A. Barcza, M. Katter, J.D. Moore, K.P. Skokov, O. Gutfleisch, Int. J. Refrig. 35 (2012) 1528.

[19] X. Chen, D.V.M. Repaka, R.V. Ramanujan, J. Alloys Compd. 658 (2016) 104.

[20] A.M. Aliev, A.B. Batdalov, I.K. Kamilov, V.V. Koledov, V.G. Shavrov, V.D. Buchelnikov, J. García, V.M. Prida, B. Hernando, Appl. Phys. Lett. 97 (2010) 212505.

[21] V. Recarte, J.I. Pérez-Landazábal, V. Sánchez-Alárcos, V.A. Chernenko, M. Ohtsuka, Appl. Phys. Lett. 95 (2009) 141908.

[22] I. Dubenko, M. Khan, A.K. Pathak, B.R. Gautam, S. Stadler, N. Ali, J. Magn. Magn. Mater. 321 (2009) 754.

[23] M.K. Chattopadhyay, V.K. Sharma, S.B. Roy, Appl. Phys. Lett. 92 (2008) 022503.

[24] J. L. Sánchez Llamazares, C. García, B. Hernando, V.M. Prida, D. Baldomir, D. Serantes, J. González, Appl. Phys. A 103 (2010) 1125.

[25] P. Czaja, W. Maziarz, J. Przewoźnik, C. Kapusta, L. Hawelek, A. Chrobak, P. Drzymała, M. Fitta, A. Kolano-Burian, J. Magn. Magn. Mater. 358–359 (2014) 142.

[26] A. Quintana-Nedelcos, J.L. Sánchez-Llamazares, D. Ríos-Jara, A.G. Lara-Rodríguez, T. García-Fernández, Phys. Status Solidi A 210 (2013) 2159.

[27] J.W. Lai, Z.G. Zheng, R. Montemayor, X.C. Zhong, Z.W. Liu, D.C. Zeng, J. Magn. Magn. Mater. 372 (2014) 86.

[28] T. Samanta, D.L. Lepkowski, A.U. Saleheen, A. Shankar, J. Prestigiacomo, I. Dubenko, A. Quetz, I.W.H. Oswald, G.T. McCandless, J.Y. Chan, P.W. Adams, D. P. Young, N. Ali, S. Stadler, Phys. Rev. B 91 (2015) 020401.

[29] T. Jaworska-Gołąb, S. Baran, R. Duraj, M. Marzec, V. Dyakonov, A. Sivachenko, Y. Tyvanchuk, H. Szymczak, A. Szytuła, J. Magn. Magn. Mater. 385 (2015) 1.

[30] C.F. Sánchez-Valdés, J.L. Sánchez Llamazares, H. Flores-Zúñiga, D. Ríos-Jara, P. Alvarez-Alonso, P. Gorria, Scr. Mater. 69 (2013) 211.

[31] T. Samanta, I. Dubenko, A. Quetz, S. Stadler, N. Ali, Appl. Phys. Lett. 101 (2012) 242405.

[32] N. T. Trung, L. Zhan, L. Caron, H.J. Buschow, E. Brück, Appl. Phys. Lett. 96 (2010) 172504.

[33] C.L. Zhang, D.H. Wang, Q.Q. Cao, Z.D. Han, H.C. Xuan, Y.W. Du, Appl. Phys. Lett. 93 (2008) 122505.

[34] J.L. Wang, P. Shamba, W.D. Hutchison, Q.F. Gu, M.F. Md Din, Q.Y. Ren, Z.X. Cheng, S.J. Kennedy, S.J. Campbell, S.X. Dou, J. Appl. Phys. 117 (2015) 17.

[35] G. Daniel-Pérez, J.L. Sánchez Llamazares, A. Quintana-Nedelcos, P. Álvarez-Alonso, R. Varga, V. Chernenko, J. Appl. Phys. 115 (2014) 17A920.

[36] R. Wu, F. Shen, F. Hu, J. Wang, L. Bao, L. Zhang, Y. Liu, Y. Zhao, F. Liang, W. Zuo, J. Sun, B. Shen, Sci. Rep. 6 (2016) 20993.

[37] T. Samanta, I. Dubenko, A. Quetz, S. Stadler, N. Ali, J. Magn. Magn. Mater. 330 (2013) 88.

[38] A. Quintana-Nedelcos, J.L. Sánchez Llamazares, H. Flores-Zúñiga, J. Alloys Compd. 644 (2015) 1003.

[39] V. Johnson, Inorg. Chem. 14 (1975) 117.

[40] N. T. Trung, First-order phase transitions and giant magnetocaloric effect, Ph.D. Thesis, Technische Universiteit Delft (ISBN/EAN: 978-90-8593-081-5), September 2010. http://dx.doi.org/10.1063/1.3399773.

[41] T. Kanomata, H. Ishigaki, T. Suzuki, H. Yoshida, S. Abe, T. Kaneko, J. Magn. Magn. Mater. 140–144 (1995) 131.

[42] S. Niziol, A. Bombik, W. Bazela, A. Szytula, D. Fruchart, J. Magn. Magn. Mater. 27 (1982) 281.

[43] K. Koyama, M. Sakai, T. Kanomata, and K. Watanabe, Jpn. J. Appl. Phys., 43 (2004) 8036.

[44] M.E. Wood, W. H. Potter, Cryogenics 25 (1985) 667.

[45] L. Caron, N.T. Trung, E. Brück, Phys. Rev. B 84 (2011) 020414.

[46] N.T. Trung, V. Biharie, L. Zhang, L. Caron, K.H.J. Buschow, E. Brück, Appl. Phys. Lett. 96, (2010) 162507.

[47] E.K. Liu, W. Zhu, L. Feng, J.L. Chen, W.H. Wang, G.H. Wu, H.Y. Liu, F.B. Meng, H.Z. Luo, Y.X. Li, Europhys. Lett. 91 (2010) 17003.

FIGURE CAPTIONS

Figure 1. (left column) and Figure 2 (right column). (a) heating/cooling DSC curves. (b) $M_{ZFC}(T)$ and $M_{FC}(T)$ curves measured under $\mu_o H = 5$ mT. (c) $\Delta S_T(T)$ curve obtained from isothermal magnetization $M(\mu_o H)$ curves measured following thermal protocols TP-1 and TP-2, respectively. The solid circles and diamonds indicate the measurement route followed in each case. In the case of TP-1 an arrow from solid circle to solid rhombus indicate the initial and final state of the field induced phase transition (FIPT) for each isotherm. The Curie temperature of the hexagonal phase is pointed out by arrows on the $M(T)$ curves. The vertical white stripe depicted in figures 1 and 2 denotes the temperature interval in which the total field induced magnetic entropy change was calculated (see text for details).

Figure 3. Room-temperature X-ray powder diffraction patterns for $MnCoGeB_{0.01}$ ribbons (a) after cooling down to 77 K and (b) after heating up to 1148 K.

Figure 4. Set of isothermal magnetization $M(\mu_o H)$ curves measured on increasing the applied magnetic field up to 5 T for $MnCoGeB_{0.01}$ alloy ribbons following thermal procedures TP-1 (a) and TP-2 (c). The field up and field down $M(\mu_o H)$ curves (up to 2 T) for selected temperatures measured following TP-1 (b) and TP-2 (d).
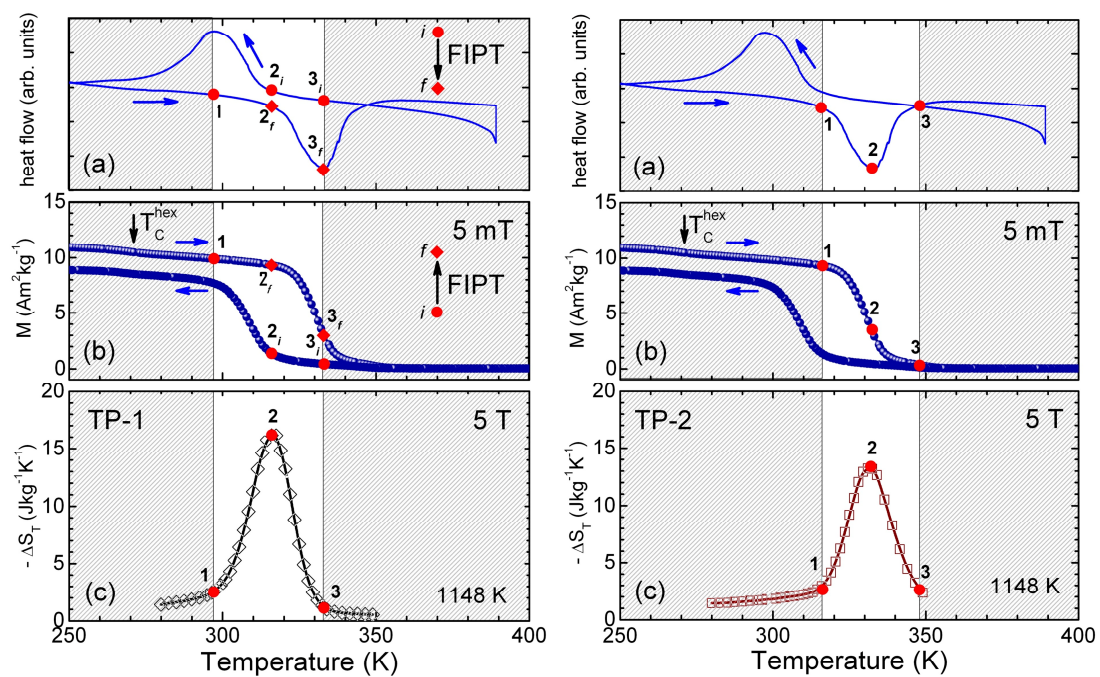
Figure 5. RC-1, RC-2 and RC-3 as a function of $\mu_o \Delta H$ for TP-1 (a) and TP-2 (b).
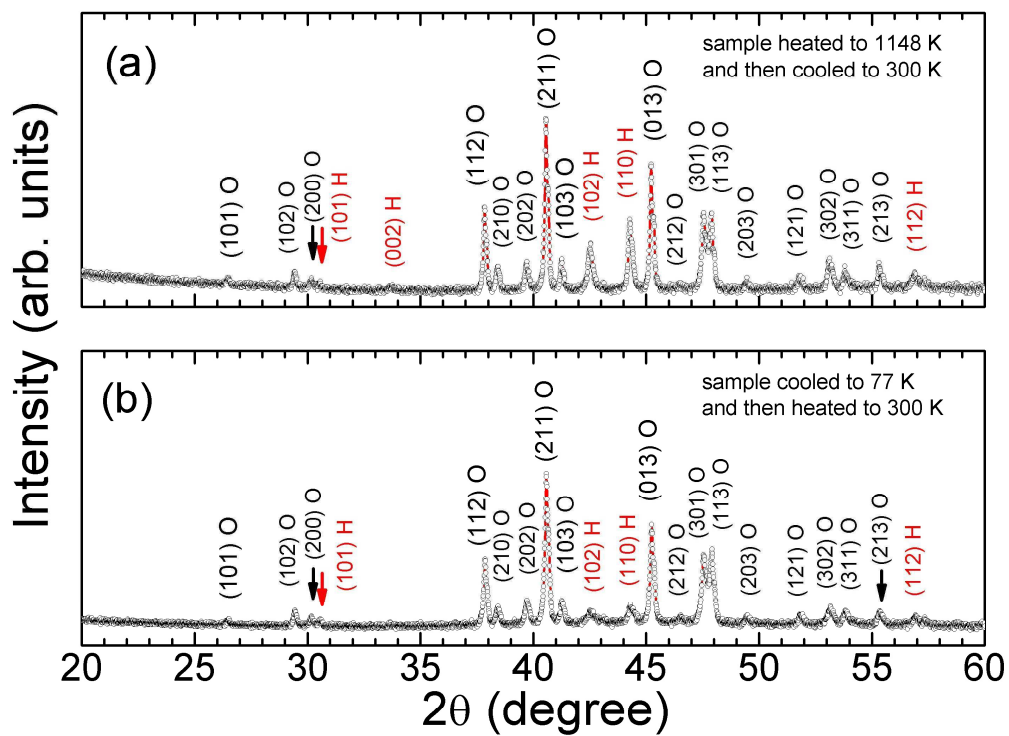
Figure 6. $M(T)$ curves at 5 T obtained from isofield measurement and from $M(\mu_o H)$ curves following thermal procedures TP-1 and TP-2.
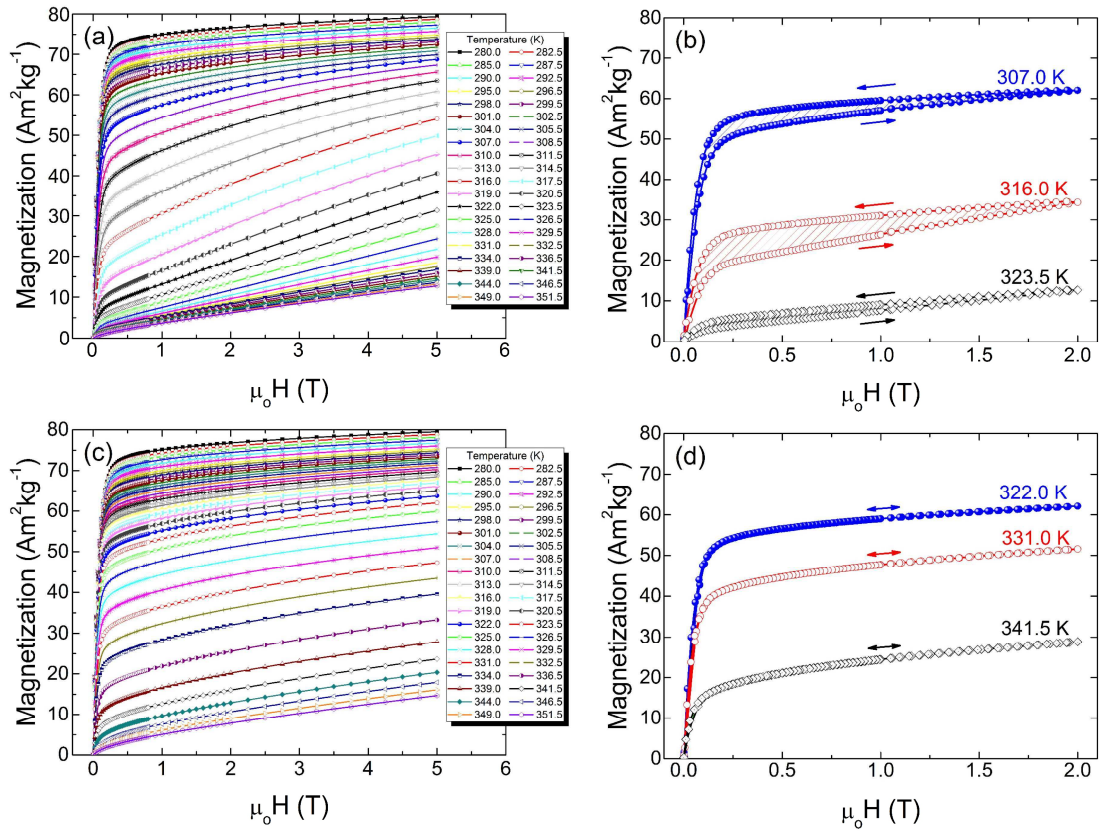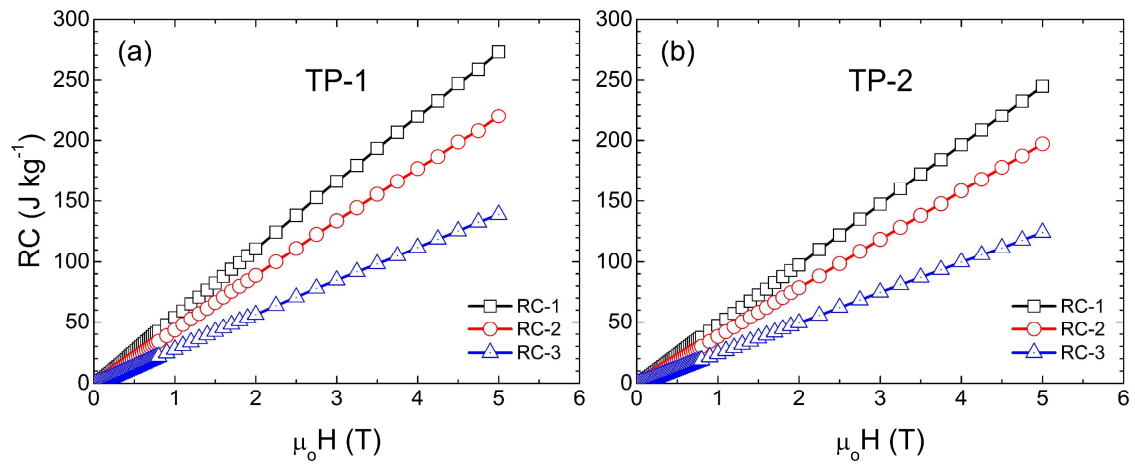
TABLE CAPTION

Table 1. Values of RC-1, RC-2 and RC-3 calculated for magnetic field changes $\mu_o \Delta H$ of 2 T and 5 T for thermal procedures TP-1 and TP-2.

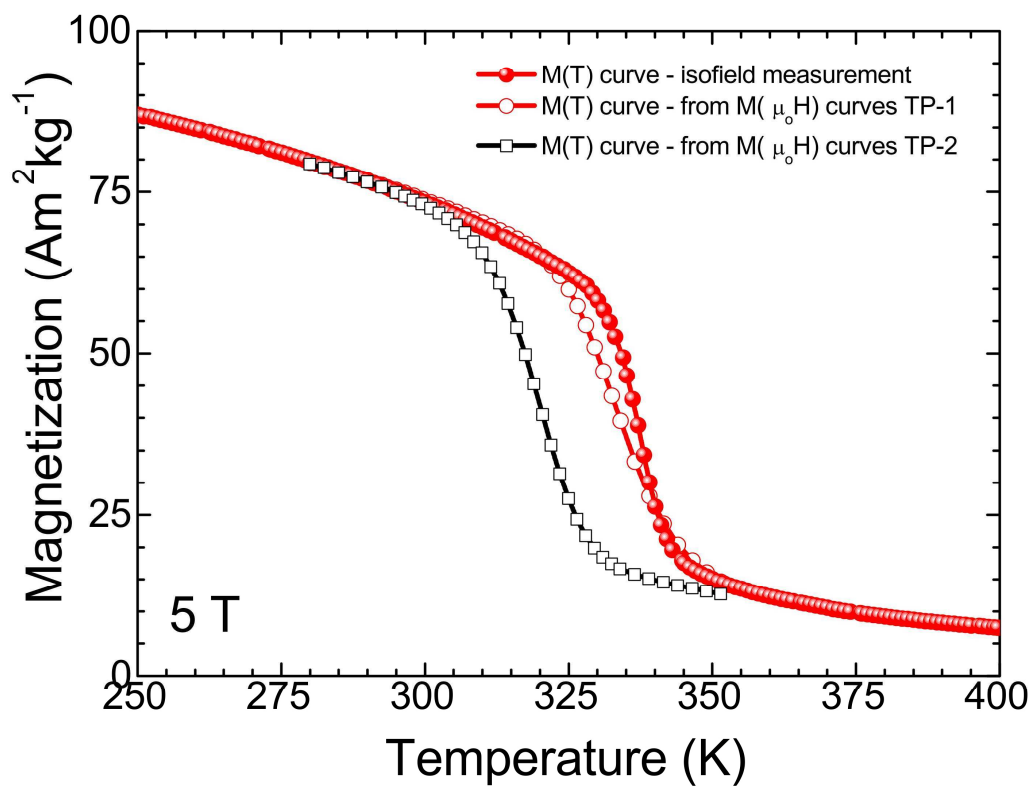| $\mu_o \Delta H$	2 T			5 T		
criteria	TP-1	TP-2	diff (%)	TP-1	TP-2	diff (%)
RC-1 (Jkg^{-1})	110	97	11.8	292	265	9.2
RC-2 (Jkg^{-1})	88	78	11.4	272	244	10.3
RC-3 (Jkg^{-1})	56	50	10.7	220	197	10.5

13

Highlights

- Correct estimation of total field induced entropy change from Maxwell relation is discussed.
- We compare results after using two different measurement procedures.
- Unidirectional measurement of isothermal magnetization curves proves to be fundamental.
- Magnetic entropy change overestimation can be avoided by using proper measurement procedure.